Science of the Total Environment 847 (2022) 157603

Contents lists available at ScienceDirect

Science of the Total Environment

journal homepage: www.elsevier.com/locate/scitotenv

A Digital Twin modelling framework for the assessment of seagrass Nature Based Solutions against storm surges

Umesh Pranavam Ayyappan Pillai [a,*], Nadia Pinardi [a], Jacopo Alessandri [a,b], Ivan Federico [c], Salvatore Causio [c], Silvia Unguendoli [b], Andrea Valentini [b], Joanna Staneva [d]

[a] Department of Physics and Astronomy, University of Bologna, Bologna 40127, Italy
[b] Hydro-Meteo-Climate Service of the Agency for Prevention, Environment and Energy of Emilia-Romagna, Arpae-SIMC, Bologna 40122, Italy
[c] Euro-Mediterranean Center on Climate Change, Lecce 73100, Italy
[d] Institute of Coastal Systems-Analysis and Modeling, Helmholtz-Zentrum Hereon, Geesthacht 21502, Germany

HIGHLIGHTS

- Digital Twin methodology can be used for testing Nature Based Solutions with seagrass meadows to protect wave attenuation and current reduction at the coasts.
- Seagrass landscaping is a key element in effectiveness of NBS seagrass wave reduction.
- Sea level reduction due to seagrass is negligible.

GRAPHICAL ABSTRACT

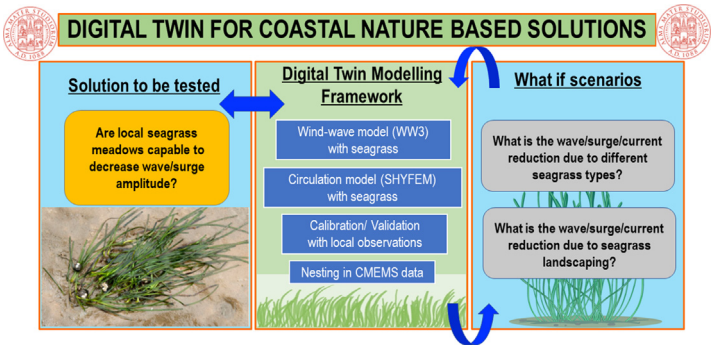

ARTICLE INFO

Guest Editor: Irene Laiz

Keywords:
Nature-based solutions
Digital Twin
Seagrass
Wave attenuation
Landscaping
Zostera marina

ABSTRACT

In this paper we demonstrate a novel framework for assessing nature-based solutions (NBSs) in coastal zones using a new suite of numerical models that provide a virtual *"replica"* of the natural environment. We design experiments that use a Digital Twin strategy to establish the wave, sea level and current attenuation due to seagrass NBSs.
This Digital Twin modelling framework allows us to answer *"what if"* scenario questions such as: (i) are indigenous seagrass meadows able to reduce the energy of storm surges, and if so how? (ii) what are the best seagrass types and their landscaping for optimal wave and current attenuation? An important result of the study is to show that the landscaping of seagrasses is an important design choice and that seagrass does not directly attenuate the sea level but the current amplitudes. This framework reveals the link between seagrass NBS and the components of the disruptive potential of storm surges (waves and sea level) and opens up new avenues for future studies.

1. Introduction

Digital Twin software systems have so far been mainly applied to industrial engineering design problems to verify that product manufacturing is closer to what is desired (Grieves, 2014; Fuller et al., 2020). The concept is based on the need to replicate the object with software that is flexible enough for continuously collected measurements and which fully exploits the capabilities of hybrid modelling (machine learning and deterministic representation of the physical object). The methodological aspects of a Digital Twin approach to studying the earth system or its sub-components have not been established, but we can start building knowledge from specific

* Corresponding author.
E-mail address: umesh.pranavam@unibo.it (U.P.A. Pillai).

http://dx.doi.org/10.1016/j.scitotenv.2022.157603
Received 31 March 2022; Received in revised form 22 June 2022; Accepted 20 July 2022
Available online 25 July 2022

application cases as we do in this article. We use deterministic ocean numerical modelling, with the aim of proposing the best design of solutions to problems such as wave attenuation and coastal erosion reduction.

The oceanographic community is developing a complex suite of deterministic numerical models, coupled and uncoupled, to replicate the natural environment, calibrating them with observations. Computational oceanography has come of age (Haine et al., 2021) and ocean models can reproduce realistic structures in the ocean so that they can be used for Digital Twin experiments. In this paper, we focus on the problem related to coastal protection by seagrass meadows, a type of nature-based solution (NBS) recognized as important for the mitigation and adaptation of coasts to the risk of climate change.

1.1. The Digital Twin for Seagrass NBSs

One third of the global coasts are geomorphologically dynamic (Luijendijk et al., 2018), since they are exposed to storms, tides, waves, and climate sea level rise (Athanasiou et al., 2020). In the offshore and nearshore regions, human activities are strongly affected by (Meucci et al., 2020) wind wave events (locally generated waves). Increased frequency/intensity of coastal risks and sea level rise related to climate change require fit-for-purpose and improved nearshore protection (Hanley et al., 2020; Ondiviela et al., 2020; Lobeto et al., 2021). In this context, the application of NBS has gained great attention, mainly due to its ability to address social, environmental and climate concerns (Nesshöver et al., 2017; Calliari et al., 2019; Kumar et al., 2020; Giordano et al., 2020; Stankovic et al., 2021; Gómez Martín et al., 2021). In recent decades, a global decline in seagrass meadows has been observed due to numerous environmental activities (Waycott et al., 2009; Donatelli et al., 2019; McKenzie et al., 2020). Furthermore, the European Union (EU) supports ecological quality levels in coastal regions (Krause-Jensen et al., 2005; Marba et al., 2013) and has established principles for the use of seagrasses as indicators of the health of the ecosystem (de los Santos et al., 2019).

This paper shows a Digital Twin framework for assessing the reduction of coastal storm surges by benthic marine vegetation such as seagrass in the coastal strip of Emilia-Romagna (ER). Two different models are used to simulate the full spectrum of processes: (i) a general circulation model considering sea level and turbulent currents, astronomical tides, atmospheric pressure, winds, temperature and salinity, including river runoff; and (ii) a wind-wave model that simulates the wave propagation and formation in offshore and coastal areas. The novelty derives from the fact that, using this Digital Twin framework, we can ask questions such as: which type of seagrass is the most effective in reducing the amplitude of the wave and of the current?; which seagrass landscaping offers an optimal solution to storm surge reduction?

1.2. Role of coastal seagrass landscapes

Seagrasses are defined as “ecosystem engineers” (Madsen et al., 2001; Denny, 2021) and include coastal ecosystems, which belong to a decidedly productive sector that provides crucial benefits (Orth et al., 2006; UNEP (United Nations Environment Programme), 2020; Young et al., 2021) such as biodiversity, nutrient cycling, etc. Seagrass meadows play a significant role in protecting coastal regions (Duarte et al., 2013; Ondiviela et al., 2014; Effrosynidis et al., 2018; Ondiviela et al., 2020) from associated flooding, erosion and storm surges. Seagrass landscapes are low-energy environments, with sediment deposition capacity (Gacia and Duarte, 2001; Ganthy et al., 2015), and which enable the resuspension of sediments (Amos et al., 2004; Widdows et al., 2008; Potouroglou et al., 2017; Zhu et al., 2021). Many studies have reported that seagrasses enable wave damping (Koch and Gust, 1999; Méndez and Losada, 2004; Paul and Amos, 2011), and modify local hydrodynamics (Fonseca and Fisher, 1986; Widdows et al., 2008; Zhang and Nepf, 2019). Water waves which propagate through submerged vegetation lose energy by performing work on the plant stems (due to plant induced forcing acting on the fluid), which directly results in smaller wave heights (Dalrymple et al., 1984) defined as “wave damping”. The seagrass beds have a high potential to alter the local hydrodynamic environment (Fonseca and Koehl, 2006) changing the velocity profile and the turbulence in the bottom boundary layer (Alessandri, 2022). Therefore, submerged vegetation such as seagrasses represent a unique ecosystem (James et al., 2019, 2021) for NBS, and eco-engineering.

Flexible seagrass leaves have a high ability to reduce flow velocity (Méndez et al., 1999; Paul and Amos, 2011), and wave energy thus promoting sedimentation (preventing erosion) and, above all, seagrass roots/rhizomes help protect the coast from erosion by maintaining sediments (Chen et al., 2007; Hendriks et al., 2008; James et al., 2021). Continuous capture and retention of sediments for longer periods can lead to complex bathymetric generation in seagrass landscape regions. Along the modified bathymetry, refraction of the waves occurs (Paul and Amos, 2011), thus leading to wave shoaling. A reduction in the orbital velocities follows the dispersion of the waves, leading to the dissipation of energy along the shoreline (Lei and Nepf, 2019). Thus the attenuation of currents and waves with seagrass leaves can trap and stabilize sediments, and the ensuing bathymetric changes aid in coastal protection (James et al., 2019). James et al. (2021), reported that seagrasses can significantly mitigate extreme storm events. In the context of climate change, the marine vegetation can adapt to sea level rise through inland migration/ soil elevation (Duarte et al., 2013).

This paper evaluates only some of the aspects of seagrass landscaping in wave reduction, i.e., the effects of seagrass distribution and of the different seagrass types in a high-fidelity replica of the coastal physical environment of the ER coasts in the Northern Adriatic Sea.

The paper is organized as follows: Section 2 describes the study site both from the point of view of the specific habitats and the numerical models implemented, Section 3 describes the calibration of the models and Section 4 the Digital Twin experiments. Section 5 provides further evidence of the impact of the NBS solution. Section 6 provides conclusions and discussions of the findings.

2. The study site

The coastal plain of Emilia-Romagna has a naturalistic and economic significance (Perini et al., 2017), with a distinct place in the tourism industry throughout Europe and therefore part of the UNESCO's “Man and Biosphere Programme”. Due to its low-slung characteristics (Armaroli et al., 2012; Armaroli and Duo, 2018; Armaroli et al., 2019), and urbanization, the ER coast is susceptible to coastal flooding (Perini et al., 2016), and erosion. The ER coast includes dissipative (low gradient) beaches comprising fine to intermediate sands (Meli et al., 2021). The prevailing storms in this coast emerge from the Bora (NE) and Scirocco winds (SE), and the coast experiences a wave height (Hs) lower than 1.25 m (low energy waves), along with microtidal regimes (Ciavola et al., 2007; Sedrati et al., 2009). The study area along the ER coast is as indicated in Fig. 1.

2.1. Seagrass in the study site

In European coastal waters, in addition to *Posidonia oceanica*, there are three native species of seagrass: *Cymodocea nodosa*, *Zostera noltii*, and *Zostera marina* (Procaccini et al., 2003; Ondiviela et al., 2014; de los Santos et al., 2019; Oprandi et al., 2020). *Zostera marina* is an abundant species in the North Sea, and in the Baltic Sea. In the Mediterranean seas it appears as isolated patches and is seen mainly in lagoons. *Zostera marina* grows up to a water depth 10–15 m and has shoots with 3–7 leaves. The width of the leaves varies from 2 mm (young plants) to 10 mm (large plants); and the leaves are about 30–60 cm long. *Zostera noltii* is found on the coasts of Norway, the Black Sea, the Mediterranean Sea and produces dense meadows on the muddy sands in the intertidal regions. They have small and narrow leaves (2–5), which are 0.5–2 mm wide and 5–25 cm long; with many shoots on each rhizome (Borum et al., 2004; Ondiviela et al., 2014). *Cymodocea nodosa* is a warm water species widespread in the Mediterranean, on the African coast (to the north) and in the Canary

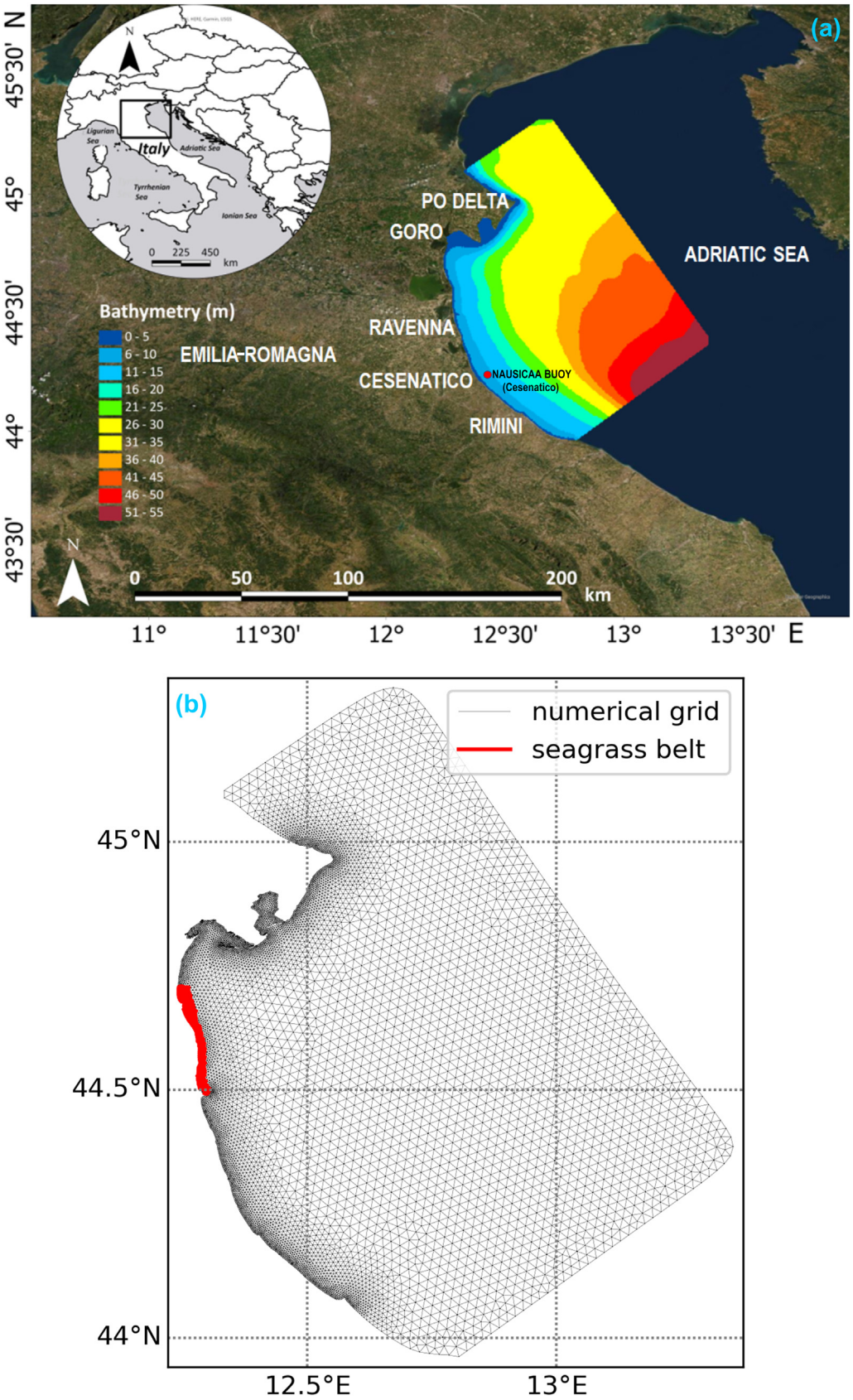

Fig. 1. (a) Coastal belt of Emilia-Romagna: map showing the study domain with bathymetry and (b) model spatial grid with oceanic nodes (black points) and the position of the seagrass belt (red strip).

Islands. It occurs mainly in the sub-tidal (shallow) regions up to deeper waters (50 to 60 m). This species shows bundles of leaves with 2–5 leaves, 2–4 mm wide and 10–4 cm long. *Posidonia oceanica* is restricted to the Mediterranean, and is found in the subtidal regions near the coast up to depths of 50–60 m. It has leaf bundles with 5–10 leaves, broad (5–12 mm), and 20–40 cm long leaves (Borum et al., 2004).

In the past, losses and recoveries of marine seagrass in Europe have been observed (Telesca et al., 2015), with a decreasing trend mainly for *Posidonia oceanica*, which suffered losses of about 13–50 % (de los Santos et al., 2019). In the Mediterranean, the distribution of *Zostera marina* is sparse, since the species is unable to adapt to the prevailing local climate (Curiel et al., 1997). However, in the northern Adriatic coasts, *Zostera marina* exists with climatic/ environmental conditions (temperature, salinity, tidal range, etc.) similar to those prevailing (Sacchi et al., 1990) in the northern Atlantic coasts. The frequent occurrence of *Zostera marina* along the ER coastal belt has been reported in a study by Pergent et al. (2014).

The NBS implemented in this study is located in the coastal strip of Emilia-Romagna (Italy).

2.2. Digital twin models

In the Digital Twin framework, we use two different types of models: a wind-wave model and an oceanographic circulation model.

The first model of interest is the WW3 wind wave model (WW3DG, 2016) which integrates a balance equation for the wave action density spectrum. This model solves for the significant wave height (Hs), wave direction, wave mean and peak period and the Stokes velocities induced by the wave motion. It is normally built for resolutions of the order of tens of meters, i.e., the same grid as the hydrodynamic current model. The WW3 model was modified to include a modified bottom dissipation stress due to submerged vegetation, thereby incorporating NBS as a potential mechanism for wave amplitude reduction.

The second model is the circulation model called SHYFEM which includes all the thermodynamic and hydrodynamic processes that contribute to the dynamics up to horizontal scales of tens of meters, several cm vertically and time scales of a few hours. SHYFEM (Umgiesser et al., 2004; Bellafiore and Umgiesser, 2009; Micaletto et al., 2021) is an unstructured finite-element model that simulates ocean circulation from the regional to the local scale worldwide (Maicu et al., 2021; Park et al., 2022), as well as in operational (Federico et al., 2017) and relocability (Trotta et al., 2021) modes. SHYFEM considers a non-time dependent coastline and sea bottom in which boundary layers are formed to dissipate mechanical energy. Hydrodynamic models of this type normally provide the best estimates of sea level as they integrate an explicit tendency equation for sea surface height. This model has been modified to include the numerical representation of seagrasses as described in Section 2.2.2.

2.2.1. Model setup

The WW3 model grid (Fig. 1) comprises 15,392 elements, connected with 8148 nodes. At the coast the resolution is about 300 m, while at the open boundary it is 2.5 km (Fig. 1b). The bathymetry of the ER domain merges high resolution multibeam measurements (from the ER regional Environmental Agency - Arpae), together with the European Marine Observation and Data Network (EMODnet) dataset, that has a resolution of about 250 m (Fig. 1a). The model spectrum covers 30 frequencies (0.0500–0.7932 Hz), and 24 directions (with an increment factor of 1.1). The time steps for the WW3 model are set as: (i) maximum global time step: 200 s, (ii) maximum CFL time step X-Y: 50 s, (iii) maximum CFL time step k-theta: 50 s, and (iv) minimum source term time step: 10 s. The linear and wind input source term uses the parameterization defined by Cavaleri and Malanotte-Rizzoli (1981), and Donelan et al. (2006). The ST6 physics is used as the wind input/dissipation parameterization (Zieger et al., 2015). To simulate the non-linear interactions (Tolman, 2014), the Generalized Multiple DIA (GMD) was used. The physics of Battjes and Janssen (1978) is used to activate breaking (depth-induced). The dissipation physics used the formulations by Rogers et al. (2012), and adapted formulations by Ardhuin et al. (2003) to simulate the SHOWEX (Shoaling Waves Experiment) bottom friction. SHOWEX parameterization can be defined as a ripple-induced bottom friction, considering the formation of sand ripples (on the bottom).

ECMWF analysis winds (with a horizontal resolution of 0.125°) is used to force the WW3 model (every 6 h). The lateral wave boundary values (with a resolution of 4.5 km hourly) are used from the CMEMS service (Copernicus Marine Environment Monitoring Service, https://marine.copernicus.eu) (Korres et al., 2021). On the basis of the CMEMS wave parameters (Hs, peak period, and mean direction) the nodes at the open boundary are forced with JONSWAP wave spectrum (Yamaguchi, 1984) approximation.

The grid, bathymetry, and input winds of the SHYFEM domain are the same as the WW3 model. The vertical space is represented with 28 z levels/ layers with a thickness of 2 m up to a maximum depth of 55 m. Vertical mixing is parameterized with a k-epsilon turbulence closure model from the state-of-the-art model GOTM (Burchard et al., 1999). The horizontal viscosity is calculated using the Smagorinsky formulation with a background kinematic viscosity of 0.2 m^2/s. The horizontal and vertical advection for active tracers uses an upwind scheme. The bottom friction is parameterized with a quadratic formulation and the definition of a roughness length. Air-sea interactions are parameterized with specific bulk formulas (Pettenuzzo et al., 2010). At the open ocean lateral boundary of the domain, ocean variables from CMEMS reanalysis (Escudier et al., 2020) are used for zonal current velocity, meridional current velocity, sea level, temperature, and salinity.

2.2.2. Inserting vegetation drag effects in the digital twin models

For WW3, the SHOWEX (Ardhuin et al., 2003) bottom friction formulation is used. The source term is described as;

$$S_{bot}(k,\theta) = -f_e u_b \frac{\sigma^2}{2g\ sinh^2(kd)} N(k,\theta) \quad (1)$$

where f_e is a dissipation factor, u_b is the root mean square of the bottom orbital velocity, the wave number k, the direction θ, d is mean water depth, σ is the frequency, and $N(k, \theta)$ is the wave action density spectrum.

To modify the Eq. (1) by incorporating the dissipation due to vegetation we adopted the wave damping equation due to vegetation ($S_{ds,veg}$; Dalrymple et al., 1984; Méndez and Losada, 2004) as available in the nearshore model SWAN (Simulating WAves Nearshore, Booij et al., 1999), as indicated below;

$$S_{ds,veg} = -\sqrt{\frac{2}{\pi}} g^2 \widetilde{C_D}\, b_v\, N_v \left(\frac{\tilde{k}}{\tilde{\sigma}}\right)^3 \frac{\sinh^3\tilde{k}ah + 3\ \sinh\tilde{k}ah}{3k\ \cosh^3\tilde{k}h} \sqrt{E_{tot}}\, E(\sigma,\theta) \quad (2)$$

where $\widetilde{C_D}$ is the bulk drag coefficient that may depend on the wave height, bv is the stem diameter plant, Nv is the number of plants per square meter, ah is the vegetation height, h is the water depth, $\tilde{k}$ is the mean wave number, $\tilde{\sigma}$ is the mean frequency, E_{tot} is the total wave energy, and $E(\sigma, \theta)$ is the wave variance spectrum. Note that the movement of vegetation, such as swaying, is neglected in Eq. (2).

The total bottom friction (S_t) is redefined by adding SHOWEX bottom friction (S_{bot}), with the $S_{ds,veg}$ along with a mask for the vegetation at the nodes as indicated in Eq. (3).

$$S_t = S_{bot} + Maskveg \times S_{ds,veg} \quad (3)$$

where *Maskveg* is a 2-dimensional field of values corresponding to grid nodes with vegetation (values of 1) and without (value 0).

In SHYFEM, seagrass was implemented in the governing equations following an approach similar to the ones described in Beudin et al. (2017), and Zhang et al. (2019). The seagrass form drag was written as:

$$F_{veg,x} = \frac{1}{2} C_{Dv} D_v N_v \left|\vec{u}\right| u \quad (4)$$

$$F_{veg,y} = \frac{1}{2} C_{Dv} D_v N_v \left|\vec{u}\right| v \quad (5)$$

where C_{Dv} is a plant drag coefficient, with values that can vary from close to zero to 3 (Nepf and Vivoni, 2000; Tanino and Nepf, 2008), D_v is the stem diameter, N_v is the vegetation density (number of stems per m^2), u and v are the zonal and meridional components of the velocity, respectively, and $\vec{u}$ is the velocity vector.

3. Model calibration

Model calibration is an important step in the Digital Twin methodology. Indeed, it should evolve towards real-time corrections of model solutions as done in ocean forecasting services (Ciliberti et al., 2021). However, it is still too early to apply data assimilation to coastal modelling for both physical oceanographic variables and vegetation because observations are still very limited. Therefore, our approach considers comparisons with available data, also called validation and calibration of model parameterizations instead of field state variable corrections.

3.1. Wave model calibration

The calibration/validation of the WW3 model was carried out for a 10-year period (2010–2019) and sensitivity experiments were also attempted to evaluate the performance of the model. The study entailed simulation experiments using the various wind-input dissipation source packages namely ST4 (Ardhuin et al., 2010) and ST6 physics (Babanin, 2011; Rogers et al., 2012; Zieger et al., 2015). Furthermore, the bottom friction formulations, i.e. the JONSWAP (Joint North Sea Wave Project) parameterization (Hasselmann et al., 1973) and the SHOWEX formulation (Ardhuin et al., 2003) for the sandy bottoms available in the model were tested through a series of simulations to arrive at the best formulations for the ER coastal strip. The combination of ST6 + SHOWEX gave a better performance in the coastal strip.

To evaluate the results of the model, data from the directional wave rider buoy from the Nausicaa buoy in Cesenatico (44.21°N, 12.47°E; see Fig. 1a for location), made available by Arpae, were used. The model simulated significant wave parameters, i.e. wave height (Hs), mean wave period, peak wave period and wave direction were compared with the buoy observations. The model skills were also evaluated using statistical indicators (Table 1) such as correlation coefficient (R), bias, and root mean square error (RMSE). The simulated Hs are in relatively good agreement with measurements with a correlation of 0.90 for the 10 years. Comparisons of significant wave parameters provide high confidence that the WW3 model setup is capable of reproducing wave characteristics at the study location as shown in Table 1. Due to the unavailability of the measurements, validations of the wave spectra were not possible at the study site.

Table 1
Statistics of the comparison of buoy measurements (Cesenatico) with model results.

Parameters	Statistics (2010–19)		
	R	Bias	RMSE
Significant wave height (m)	0.90	−0.05	0.21
Mean wave period (s)	0.75	−0.22	0.85
Peak wave period (s)	0.61	−0.19	1.65

R: Correlation, RMSE: Root Mean Square Error.

3.2. Circulation model validation

The circulation model parameterizations such as bottom stress drag coefficients and turbulent diffusion coefficients are calibrated with sensitivity simulations to obtain the solutions closest to the observations (Alessandri, 2022). The model was calibrated/validated with respect to observations of sea level, temperature, and salinity observations in Porto Garibaldi (near point 1 in Fig. 8b).

Validation of the model for the 10 years as indicated in Table 2 showed correlations of 0.69, 0.71 and 0.98 for sea level, salinity and temperature respectively. Salinity and temperature have mean absolute error (MAE) of 2.93 psu and 1.82 °C respectively (Alessandri, 2022).

4. Seagrass effects: the Digital Twin framework at work

We used the wave model to define the selection criteria for most impacting seagrass species and landscape designs. This allowed identifying the key NBS design choices that give maximum wave attenuation under the assumption that this is the main effect on storm surge induced coastal erosion. As a first step, experiments with *Cymodocea nodosa* and *Zostera marina* were attempted to understand if the type of seagrass was important in wave reduction. Furthermore, the sensitivity of the spatial distribution of seagrass landscapes was tested. Coppa et al. (2019) reported the striped landscape pattern (as narrow and long strips) of *Posidonia oceanica* in shallow waters of depths of 0.5 to 3 m. A low density, and high-density cluster design of landscape vegetation was also reported by Alsaffar et al. (2020).

In Danovaro et al. (2020) in the North Adriatic, a 40-year period showed a decrease in seagrasses compared to 2007–2013 period. The seagrass exists as patches, and not as continuous meadows along coastal regions. Therefore, in this study the seagrass landscaping was designed to reproduce the natural distribution of seagrass as evident from satellite images, from 2 m to 10 m depth (Fig. 1b), to avoid a position too close to the shoreline and to allow sunlight to penetrate the coastal waters.

The *Zostera marina* seagrass species selected for the coast was applied in different landscape designs as shown in Fig. 2. The four different types of landscape (LS) designs implemented are:

- Native – continuous mask (denoted as LS1)
- Lower density clusters (three-four nodes clusters, denoted as LS2)
- Continuous strips along with clusters (denoted as LS3)
- Broken strips along with clusters (denoted as LS4)

The physical characteristics of the *Cymodocea nodosa* and *Zostera marina* bed (shoot density, blade length, and width) used in the experiments are indicated in Table 3 as adopted from Mazzella et al. (1998). The bulk drag coefficient (Cd) used in (2) is 0.01.

The EXP1 is the simulation without vegetation. The EXP2 indicated in Table 3 used the CN1 vegetation along with the LS1 type seagrass mask as indicated in Fig. 2a. The EXP3 comprises a combination of the same LS1 mask along with ZM1. Fig. 3 shows the spatial plot of Hs for a selected day (25 January 2017, 12:00 h) without and with vegetation (using CN1 and ZM1) with the LS1 arrangement.

From Fig. 3a, it is seen that Hs > 1 m in the nearshore belt without vegetation. Figs. 3b & c shows the simulated Hs with the two types of vegetation and a greater reduction in Hs occurs with *Zostera marina*. To test the

Table 2
Statistics evaluated by comparing observations with circulation model results.

Parameters	Statistics (2010–19)			
	R	RMSE		MAE
Sea level (m)	0.69	0.1		0.08
	R	Bias	RMSE	MAE
Salinity (psu)	0.71	1.58	3.89	2.93
Temperature (°C)	0.98	−1.65	2.29	1.82

R: Correlation, RMSE: Root Mean Square Error, MAE: Mean Absolute Error.

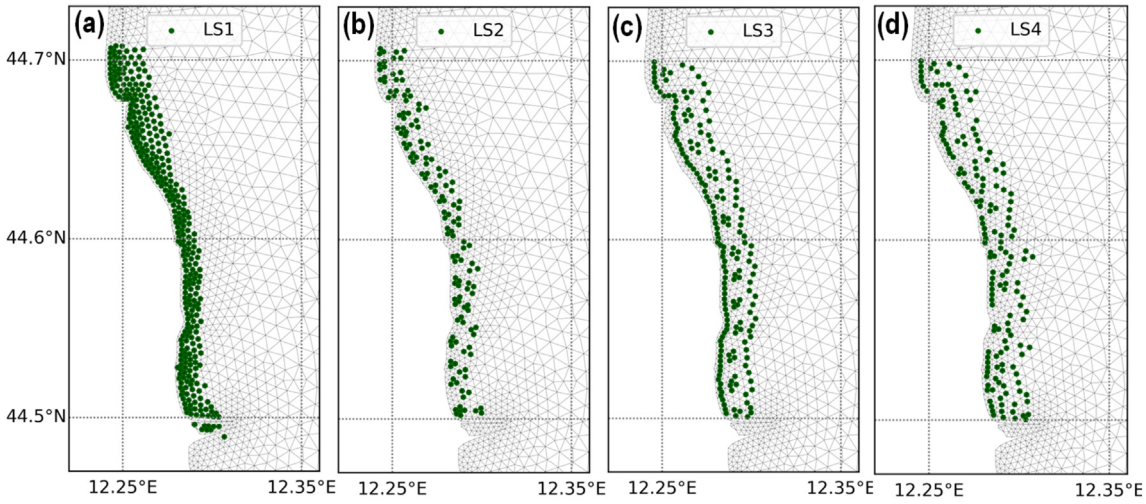

Fig. 2. Seagrass landscape designs (a) LS1: continuous mask, (b) LS2: lower density cluster, (c) LS3: continuous stripes with clusters, and (d) LS4: broken strips with clusters (green dots denotes seagrass nodes).

sensitivity of the wave spectra to the seagrass type, Fig. 4 compares the wave spectra with the uniform distributions of *Cymodocea nodosa* and *Zostera marina* (based on EXP1, 2 & 3). At station 1, during 25th day of January and March 2017, *Zostera marina* was able to produce the maximum reduction in energy compared to *Cymodocea nodosa*. Similarly, at station 2, short period waves are completely attenuated with greater attenuation using *Zostera marina*.

The landscaping experiments were thus performed using only *Zostera marina* as indicated in Table 3. Fig. 5 compares the wave spectra with different distributions of *Zostera marina* (LS2, LS3 and LS4) i.e., EXP4, EXP5 and EXP6 for January and March 2017.

Note that the short period waves (Fig. 5) are completely dissipated for all three seagrass landscapes (LS2, LS3 and LS4) with higher attenuations obtained with the broken strips along with the cluster arrangement (LS4).

The study also performed EXP7, which is a combination of *Cymodocea nodosa* with the LS4 arrangement, and showed less impact on wave attenuation than EXP6, which reaffirms our results that *Zostera marina* is best suited to the ER coastal strip along with the LS4 combination. The further results discussed in the paper are based on the combination of LS4 (broken strips together with clusters) and *Zostera marina*.

5. How good is the NBS solution?

5.1. Evaluation of wave attenuation for a 10-year period

Based on the 2017 sensitivity experiments, using the broken strips together with the clusters combined with *Zostera marina*, simulations were performed over a long period (2010–19) to increase the statistical significance of the results.

The percentage rate of wave attenuation is defined by:

$$a = \frac{h_m^{sg} - h_m^{nsg}}{h_m^{nsg}} \times 100 \quad (6)$$

where h_m^{sg} is the mean wave height with seagrass, and h_m^{nsg} is the mean wave height without seagrass.

Fig. 6(a-j) compares Hs with and without vegetation at station 2 for the period 2010–19. The mean Hs for 2010–19 was 0.19 m and 0.37 m, with and without vegetation, respectively. The Hs ranged from 0.004 to 2.04 m without vegetation, and for the case with vegetation, it ranged from 0.004 to 1.44 m. The results in Fig. 6 highlight that a significant reduction in Hs was obtained for the higher wave height ranges with the application of seagrasses in the coastal strip.

The variability of Hs using the *Zostera marina* and broken strips with clusters in two stations for 2010–2019 is shown in Fig. 7. At station 1, the percentage variation in Hs ranged from 20 to 74 % with a mean of 55 %. During the winter the attenuation was between 49 and 74 %; while in summer it ranged from 23 to 67 %. The lowest attenuation was recorded in June 2012 (20 %), but an increase has been noted since 2014. At station 2, the attenuation ranged from 6 to 68 % with a mean of 41 %. During the winter the attenuation was between 37 and 67 %; while in summer it ranged from 12 to 52 %. Similar to Station 1, the lowest attenuation was observed in June (6 %), but for the year 2013, followed by an increase for

Table 3
Seagrass scenarios and seagrass characteristics as adapted from Mazzella et al. (1998).

Experiment name	Wave Model parameters				
	Seagrass Type	Seagrass distribution	Stem diameter of plant cylinder (*Bv* in m)	No. of plants per square meter (*Nv*)	Length of seagrass (*Lv* in m)
EXP1	Without vegetation				
EXP2	*Cymodocea nodosa* (CN1)	LS1: Continuous (2-10 m)	0.0018	900	0.074
EXP3	*Zostera marina* (ZM1)	LS1: Continuous (2-10 m)	0.0038	270	0.213
EXP4	*Zostera marina* (ZM2)	LS2: Low density clusters (2-10 m)	0.0038	270	0.213
EXP5	*Zostera marina* (ZM3)	LS3: Continuous strips along with clusters (2-10 m)	0.0038	270	0.213
EXP6	*Zostera marina* (ZM4)	LS4: Broken strips along with clusters (2-10 m)	0.0038	270	0.213
EXP7	*Cymodocea nodosa* (CN2)	LS4: Broken strips along with clusters (2-10 m)	0.0018	900	0.074
		Circulation Model parameters			
ERM-CNT	Without vegetation				
ERM-SG	*Zostera marina* (ZM4)	LS4: Broken strips along with clusters (2-10 m)	0.0038	270	0.213

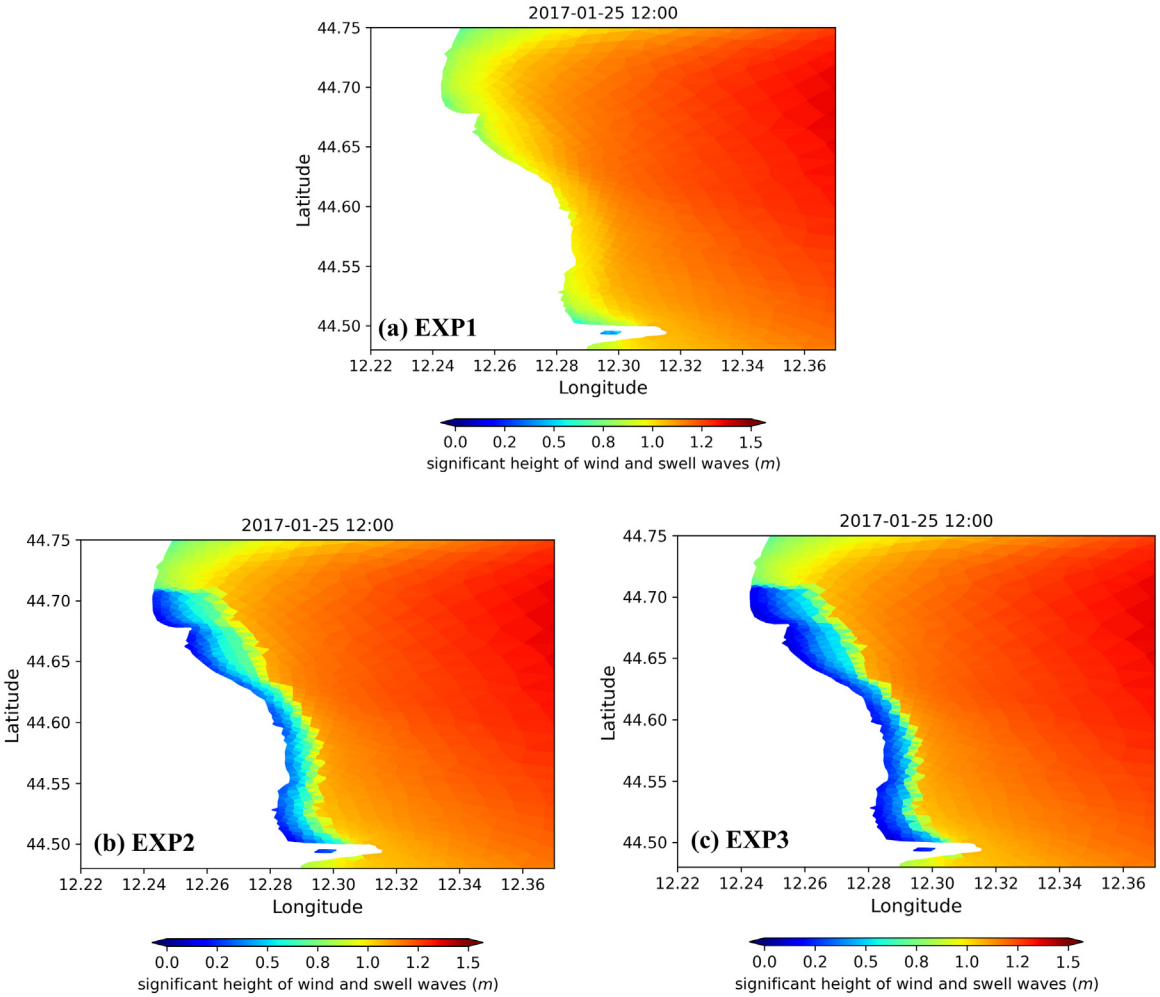

Fig. 3. Daily spatial plots of Hs (a) without vegetation, (b) with vegetation (*Cymodocea nodosa* and LS1 combination), and (c) with vegetation (*Zostera marina* and LS1 combination) for a selected day (25 January 2017, 12:00 h).

2014 to 2019. Overall, from the percentage variation of Hs in both stations considered in Fig. 7, it can be seen that there is a strong seasonality of the attenuation rates along the coastal belt. In the present simulations, the main limitation was that the simulations were performed with rigid seagrass. Future studies will thus attempt to modify the vegetation characteristics by applying advanced parameterization using flexible seagrass.

5.2. Evaluation of sea level and current velocity reduction

Having already established that wave attenuation works best with a seagrass distribution such as LS4, the SHYFEM model was used to show the impact on sea level and the current intensity.

The results (Fig. 8) are shown in terms of sea level and current velocity differences between a simulation with and without seagrass for a storm surge event due to a strong Bora wind (20–25 m/s) that occurred along the ER coast on 6 February 2015, which flooded and eroded several coastal areas. The sea level shows an increase of 1 mm NW up to the position of the seagrasses, where water accumulates due to the decrease in the amplitude of the flow, while a decrease of about 0.7–0.8 mm is observed south of the vegetated area (Fig. 8a).

In conclusion, the overall effects on the sea level appear to be negligible due to reduced length of the plant (21.3 cm) compared to the depth of the water column (between 2 and 10 m). However, a much greater impact is due to the drag exerted by the vegetation on the flow, inducing a reduction in the intensity of the current, which has its maximum at the bottom (Fig. 8b) with a reduction of up to 4–5 cm/s (~ 50 % of the currents without vegetation). The current velocity is reduced along the entire water column as shown in Fig. 9 for points 1 (left) and 2 (right) respectively, the points as indicated in Fig. 8b.

In conclusion, the reduction in amplitude of the current is effective due to seagrass while the sea level is not affected.

6. Summary and conclusions

The objective of this study was to experiment with a Digital Twin framework for the design of an optimal seagrass-based NBS for the coastal strip of Emilia-Romagna against storm surges and coastal erosion. Although the Digital Twin methodology presented here is preliminary, we believe it has great potential for coastal management. The numerical model chain consists of an ocean circulation model, and a wave model, with seagrass represented in both of them.

This study provided new insights into seagrass landscape design as an important solution characteristic to maximize the benefits. The amount of significant reduction in wave height depends on the seagrass landscaping. A combination of broken strips and clusters of vegetation has been shown to be effective in reducing wave energy on the coast compared to other landscape designs. Another important conclusion of our work is that seagrass is shown for our model configuration not to have a direct impact on sea level, but significantly reduce current amplitudes.

Since storm surges are highly dependent on wave runup (Staneva et al., 2017, 2021; Musinguzi et al., 2022) which induces coastal erosion, we believe that NBS seagrass solutions with specific landscaping of *Zostera marina* will be effective in reducing the impact of storm surges on beach erosion.

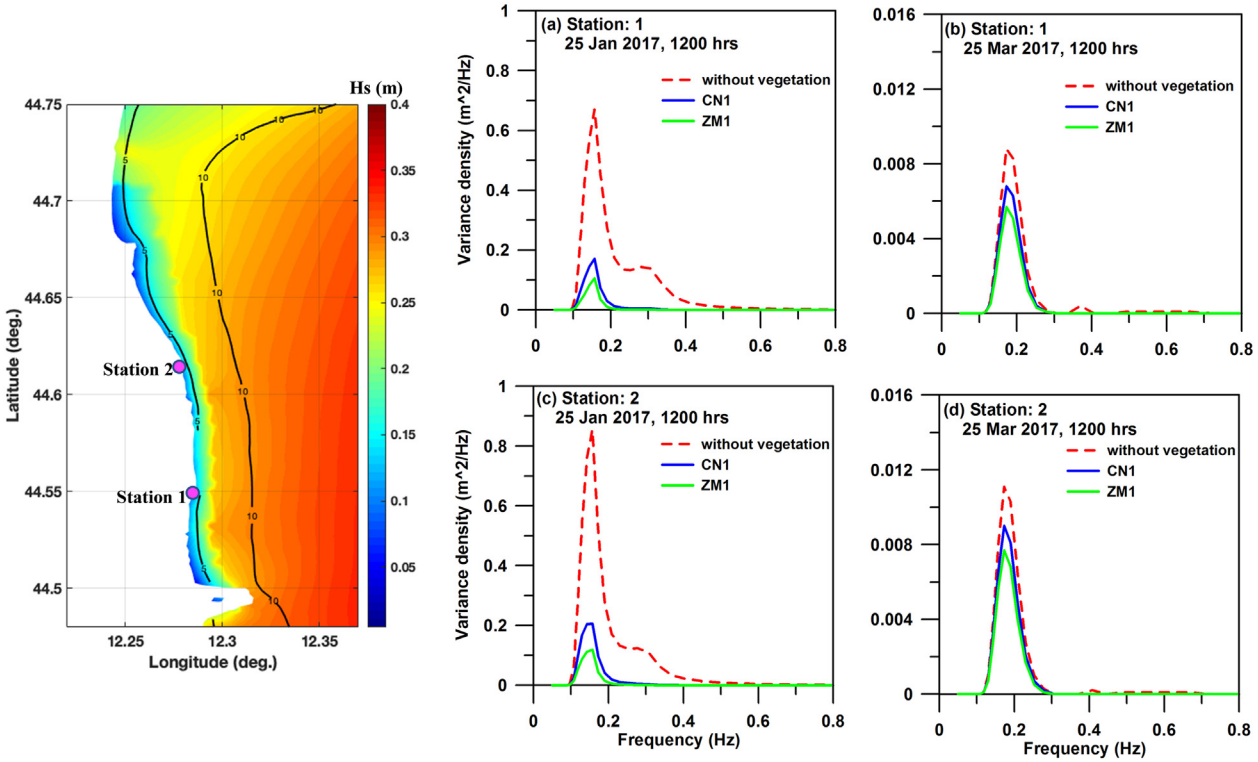

Fig. 4. Comparison of wave spectra (based on EXP1, 2 and 3) with different distributions of *Cymodocea nodosa/ Zostera marina* (for a selected day, January 25 / March 2017, 12:00 h). The map (image on the left) shows the mean Hs (in m) of March 2017 with *Zostera marina* together with the locations. In the panel (right) showing the wave spectra [a, b, c, d], the dotted red lines indicate the spectra without vegetation, continuous blue lines denote spectra with *Cymodocea nodosa* and LS1, continuous green line denotes spectra with *Zostera marina* and LS1.

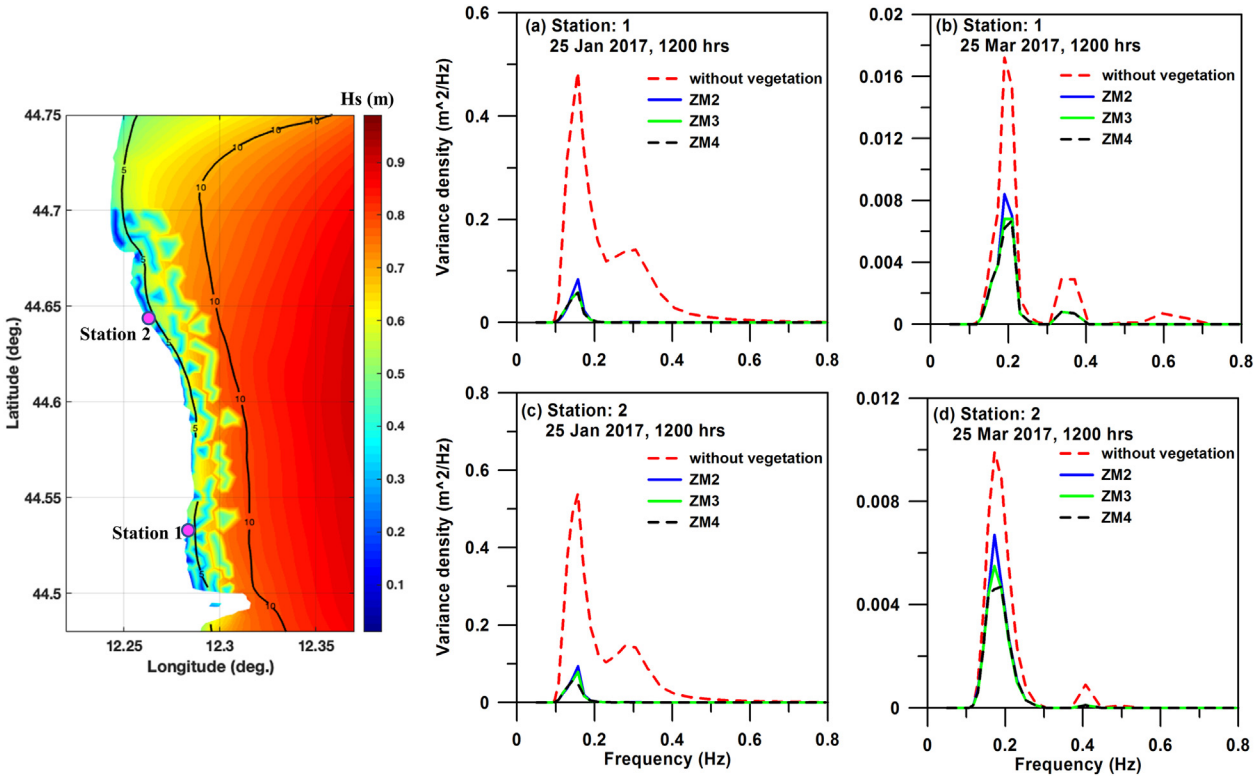

Fig. 5. Comparison of wave spectra (based on EXP1, 4, 5 and 6) with different distributions of *Zostera marina* (for a selected day, January 25 / March 2017, 12:00 h). The map (image on the left) shows the average Hs (in m) of January 2017 with *Zostera marina* together with the station locations. In the panel (right) showing the wave spectra [a, b, c, d], red dashed lines indicate the spectra without vegetation, continuous blue lines denote spectra with *Zostera marina* and LS2, the continuous green line denotes spectra with *Zostera marina* and LS3, and the black dotted line denotes the spectra with *Zostera marina* and LS4.

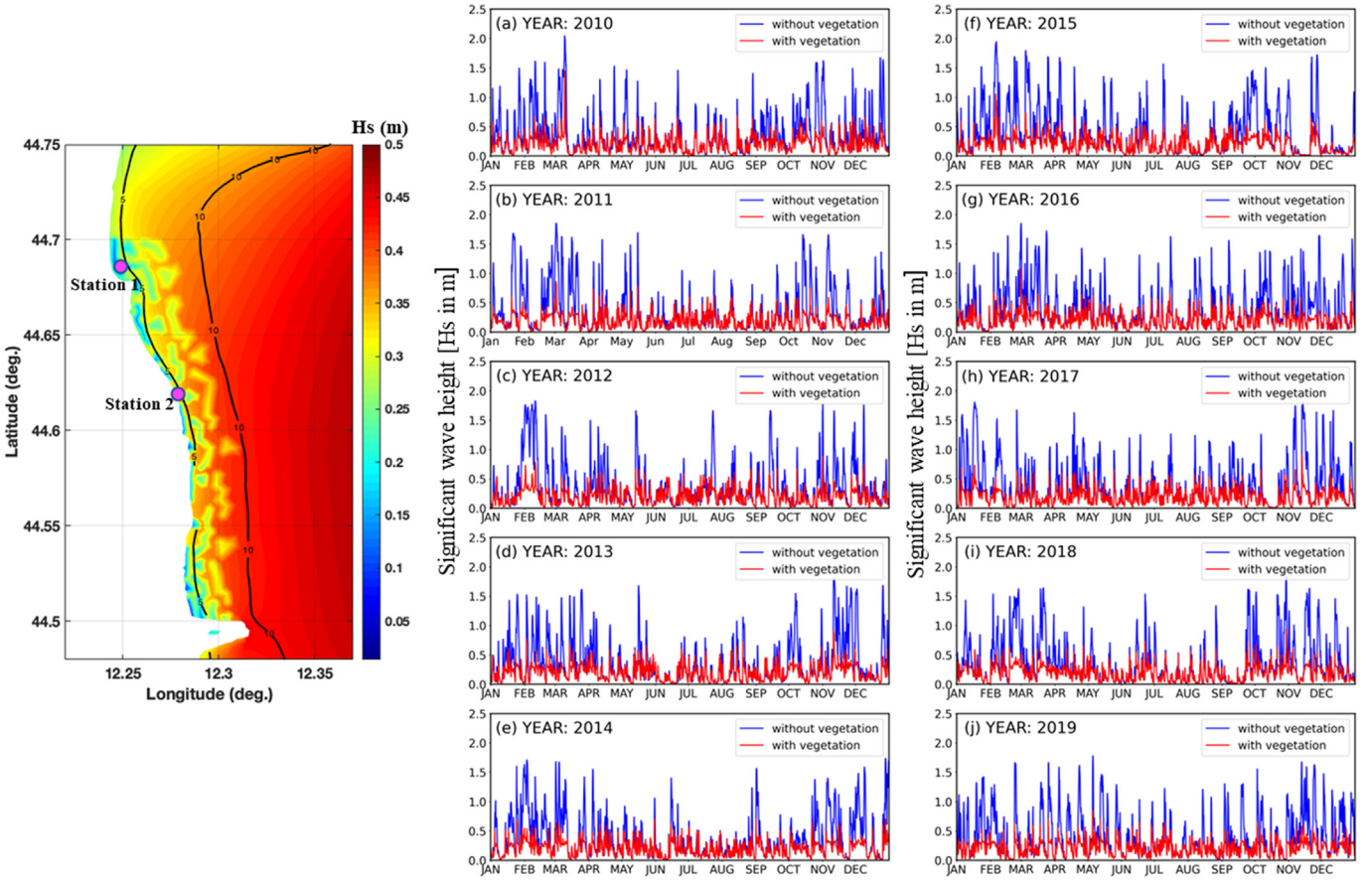

Fig. 6. Time-series comparison of wave height for the time slice 2010–2019 (a-j) at Station 2 (the blue line represents the unvegetated Hs and the red line indicates the vegetated Hs). The map (image on the left) shows the mean Hs (in m) for 2010–19 with the *Zostera marina* and LS4 combination together with the station locations.

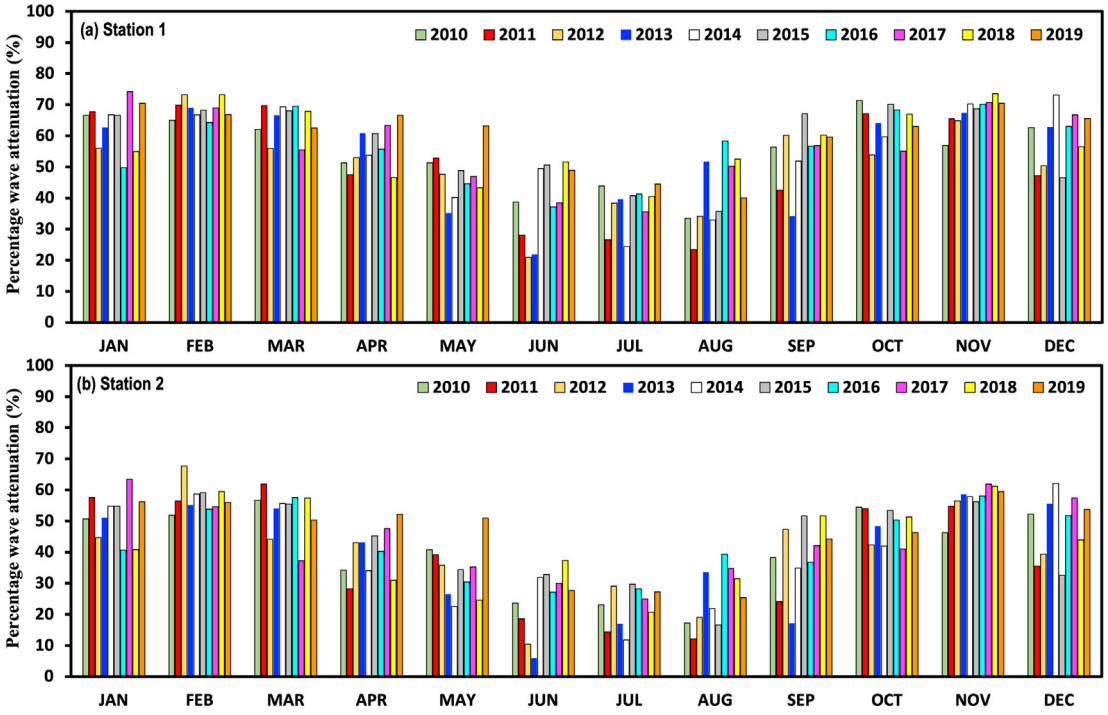

Fig. 7. Mean monthly percentage variation of wave height using *Zostera marina* and broken strips with clusters for 2010–19 (For station location, see Fig. 6.)

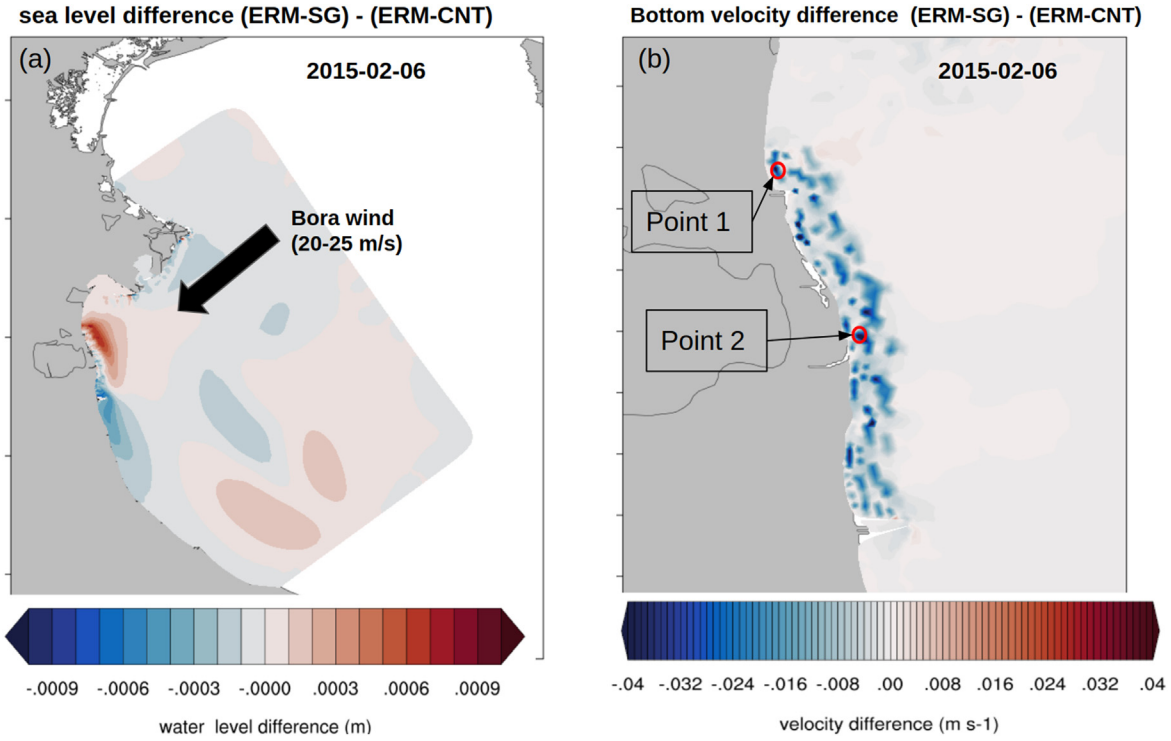

Fig. 8. (a) Sea level, and (b) bottom velocity difference between ERM-SG and ERM-CNT for the 6 February 2015. The direction and maximum intensity of the wind are presented in (a).

Overall, the study highlights that coastal vegetation has high wave attenuation capacity, however estimates to quantify wave-vegetation characteristics were not investigated as they require extensive laboratory/ field studies. Future studies could also emphasize the relevance of hyperspectral images (Clarke et al., 2021) to effectively design the landscapes on a large spatial scale. Another effect of seagrasses is connected with sediment entrapment and in the future, this should be addressed by coupling with sediment transport models.

Finally, this study shows the "Digital Twin" methodology at work and shows its potential for applications to the natural environment and to designing solutions to climate change issues such as coastal erosion and biodiversity loss. The limitations of the present Digital Twin approach are: 1) the models are still uncoupled, 2) the seagrass is still rigid, and 3) the observations are not yet assimilated into the model. For the latter, the calibration of the model parameterizations takes its place while for the model coupling, we argue that in the coastal site of Emilia-Romagna, the coupling would involve a minor simplification since the circulation currents have a relatively low amplitude. In the future, however, all these limitations should be removed, in particular the rigidity of the seagrasses.

CRediT authorship contribution statement

Conceptualization: NP, UPA, IF, SC, JA, JS; **Data curation:** UPA, IF, AV, SU; **Formal analysis:** UPA, IF, SC, JA; **Investigation:** UPA, NP, IF, SC, JA, JS; **Methodology:** NP, UPA, IF, JA, SC, SU, JS; **Project Supervision:** NP; **Validation & Visualization:** UPA, IF, SC, JA, JS; **writing original draft:** UPA, NP; **writing- review & editing:** All.

Declaration of competing interest

The authors declare that they have no known competing financial interests or personal relationships that could have appeared to influence the work reported in this paper.

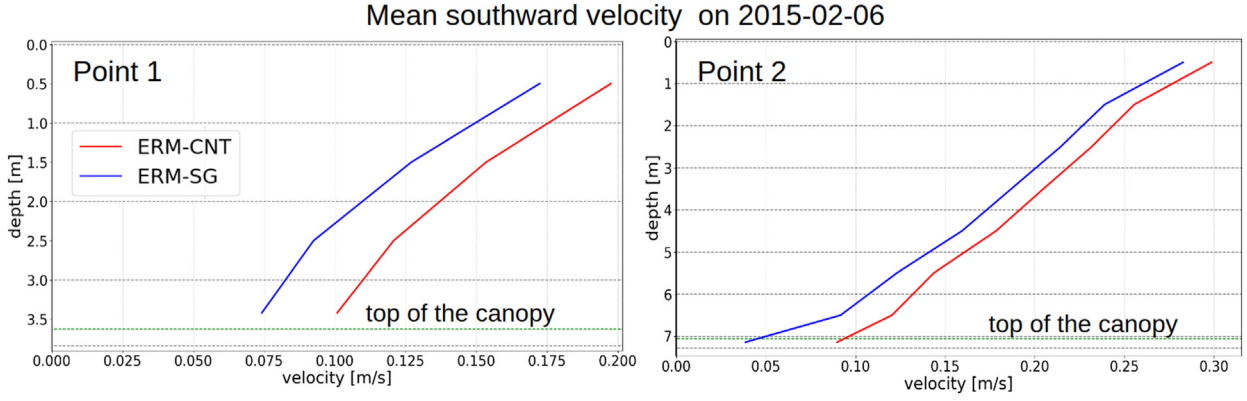

Fig. 9. Profiles of southward currents velocity with and without vegetation for point 1 (left) and point 2 (right). The position of points 1 and 2 (red circles) is indicated in Fig. 8b.

Acknowledgements

This work was carried out under the framework of OPERANDUM (OPEn-air laboRAtories for Nature baseD solUtions to Manage hydro-meteo risks) project, which is funded by the European Union's Horizon 2020 research and innovation programme under the Grant Agreement No: 776848. JS, IF, and SC acknowledges the European Green Deal project "Large scale RESToration of COASTal ecosystems through rivers to sea connectivity" (REST-COAST) (Grant No: 101037097).

References

Alessandri, J., 2022. Coastal Modelling Studies for Forecasting and Remediation Solutions. Ph.D. Thesis. University of Bologna, Italy.

Alsaffar, Z., Pearman, J.K., Cúrdia, J., Ellis, J., Calleja, M.L., Ruiz-Compean, P., Roth, F., et al., 2020. The role of seagrass vegetation and local environmental conditions in shaping benthic bacterial and macroinvertebrate communities in a tropical coastal lagoon. Sci. Rep. 10, 13550.

Amos, C.L., Bergamasco, A., Umgiesser, G., Cappucci, S., Cloutier, D., DeNat, L., Flindt, M., Bonardi, M., Cristante, S., 2004. The stability of tidal flats in Venice lagoon-the results of in-situ measurements using two benthic, annular flumes. J. Mar. Syst. 51, 211–241.

Ardhuin, F., O'Reilly, W.C., Herbers, T.H.C., Jessen, P.F., 2003. Swell transformation across the continental shelf. Part I: attenuation and directional broadening. J. Phys. Oceanogr. 33 (9), 1921–1939.

Ardhuin, F., Rogers, W.E., Babanin, A.V., Filipot, J., Magne, R., Roland, A., van der Westhuysen, A., Queffeulou, P., Lefevre, J., Aouf, L., Collard, F., 2010. Semiempirical dissipation source functions for ocean waves. Part I: definition, calibration, and validation. J. Phys. Oceanogr. 40, 1917–1941.

Armaroli, C., Duo, E., 2018. Validation of the coastal storm risk assessment framework along the Emilia-Romagna coast. Coast. Eng. 134, 159–167.

Armaroli, C., Ciavola, P., Perini, L., Calabrese, L., Lorito, S., Valentini, A., Masina, M., 2012. Critical storm thresholds for significant morphological changes and damage along the Emilia-Romagna coastline, Italy. Geomorphology 143–144, 34–51.

Armaroli, C., Duo, E., Viavattene, C., 2019. From hazard to consequences: evaluation of direct and indirect impacts of flooding along the Emilia-Romagna Coastline, Italy. Front. Earth Sci. 7, 203.

Athanasiou, P., van Dongeren, A., Giardino, A., Vousdoukas, M.I., Ranasinghe, R., Kwadijk, J., 2020. Uncertainties in projections of sandy beach erosion due to sea level rise: an analysis at the European scale. Sci. Rep. 10, 11895.

Babanin, A.V., 2011. Breaking and Dissipation of Ocean Surface Waves. Cambridge University Press, p. 480 pp.

Battjes, J.A., Janssen, J.P.F.M., 1978. Energy loss and set-up due to breaking of random waves. Proc. 16th Int. Conf. Coastal Eng. ASCE, pp. 569–587.

Bellafiore, D., Umgiesser, G., 2009. Hydrodynamic coastal processes in the north adriatic investigated with a 3d finite element model. Ocean Dyn. 60 (2), 255273.

Beudin, A., Kalra, T.S., Ganju, N.K., Warner, J.C., 2017. Development of a coupled wave-flow-vegetation interaction model. Comput. Geosci. 100, 76–86.

Booij, N., Ris, R.C., Holthuijsen, L.H., 1999. A third-generation wave model for coastal regions, part I, model description and validation. J. Geophys. Res. Oceans 104, 7649–7666.

European seagrasses: an introduction to monitoring and management. In: Borum, J., Duarte, C.M., Krause-Jensen, D., Greve, T.M. (Eds.), Monitoring and Managing of European Seagrasses Project (M&MS) ISBN 87-89143-21-3. 88 pp.

Burchard, H., Bolding, K., Villarreal, M.R., 1999. GOTM—a general ocean turbulence model. Theory, applications and test cases. Tech. Rep. EUR 18745 EN. European Commission.

Calliari, E., Staccione, A., Mysiak, J., 2019. An assessment framework for climate-proof nature-based solutions. Sci. Total Environ. 656, 691–700.

Cavaleri, L., Malanotte-Rizzoli, P., 1981. Wind-wave prediction in shallow water: theory and applications. J. Geophys. Res. 86 (C11), 10961–10973.

Chen, S.N., Sanford, L.P., Koch, E.W., Shi, F., North, E.W., 2007. A nearshore model to investigate the effects of seagrass bed geometry on wave attenuation and suspended sediment transport. Estuar. Coast. 30, 296–310.

Ciavola, P., Armaroli, C., Chiggiato, J., Valentini, A., Deserti, M., Perini, L., Luciani, P., 2007. Impact of storms along the coastline of Emilia-Romagna: the morphological signature on the Ravenna coastline (Italy). J. Coast. Res. SI50, 540–544.

Ciliberti, S.A., Grégoire, M., Staneva, J., Palazov, A., Coppini, G., Lecci, R., Peneva, E., 2021. Monitoring and forecasting the ocean state and biogeochemical processes in the Black Sea: recent developments in the Copernicus marine service. J. Mar. Sci. Eng. 9 (10), 1146.

Clarke, K., Hennessy, A., McGrath, A., Daly, R., Gaylard, S., Turner, A., Cameron, J., Lewis, M., Fernandes, M.B., 2021. Using hyperspectral imagery to investigate large-scale seagrass cover and genus distribution in a temperate coast. Sci. Rep. 11, 4182.

Coppa, S., Quattrocchi, G., Cucco, A., de Lucia, G.A., Vencato, S., Camedda, A., Domenici, P., Conforti, A., Satta, A., Tonielli, R., Bressan, M., Massaro, G., De Falco, G., 2019. Self-organisation in striped seagrass meadows affects the distributional pattern of the sessile bivalve Pinna nobilis. Sci. Rep. 9, 7220.

Curiel, D., Rismondo, A., Scarton, F., Marzocchi, M., 1997. Flowering of Zostera marina in the lagoon of Venice (North Adriatic, Italy). Bot. Mar. 40 (2), 101–105.

Dalrymple, R.A., Kirby, J.T., Hwang, P.A., 1984. Wave diffraction due to areas of energy dissipation. ASCEJ. Waterw. Port Coast. Ocean Eng. 110 (1), 67–79.

Danovaro, R., Nepote, E., Lo Martire, M., Carugati, L., Da Ros, Z., Torsani, F., Dell'Anno, A., Corinaldesi, C., 2020. Multiple declines and recoveries of Adriatic seagrass meadows over forty years of investigation. Mar. Pollut. Bull. 161 (Part B), 111804.

Denny, M., 2021. Wave-energy dissipation: seaweeds and marine plants are ecosystem engineers. Fluids 6, 151.

Donatelli, C., Ganju, N.K., Kalra, T.S., Fagherazzi, S., Leonardi, N., 2019. Changes in hydrodynamics and wave energy as a result of seagrass decline along the shoreline of a microtidal back-barrier estuary. Adv. Water Resour. 128, 183–192.

Donelan, M.A., Babanin, A.V., Young, I.R., Banner, M.L., 2006. Wave follower measurements of the wind-input spectral function. Part II. Parameterization of the wind input. J. Phys. Oceanogr. 36, 1672–1689.

Duarte, C.M., Sintes, T., Marba, N., 2013. Assessing the CO2 capture potential of seagrass restoration projects. J. Appl. Ecol. 50, 1341–1349.

Effrosynidis, D., Arampatzis, A., Sylaios, G., 2018. Seagrass detection in the mediterranean: a supervised learning approach. Ecol. Inform. 48, 158–170.

Escudier, R., Clementi, E., Omar, M., Cipollone, A., Pistoia, J., Aydogdu, A., Drudi, M., Grandi, A., Lyubartsev, V., Lecci, R., Cretí, S., Masina, S., Coppini, G., Pinardi, N., 2020. Mediterranean Sea Physical Reanalysis (CMEMS MED-Currents) (Version 1) set. Copernicus Monitoring Environment Marine Service (CMEMS). https://doi.org/10.25423/CMCC/MEDSEA_MULTIYEAR_PHY_006_004_E3R1.

Federico, I., Pinardi, N., Coppini, G., Oddo, P., Lecci, R., Mossa, M., 2017. Coastal Ocean forecasting with an unstructured grid model in the southern adriatic and northern ionian seas. Nat. Hazards Earth Syst. Sci. 17 (1), 4559.

Fonseca, M.S., Fisher, J.S., 1986. A comparison of canopy friction and seagrass movement between four species of seagrass with reference to their ecological restoration. Mar. Ecol. 29, 15–22.

Fonseca, M.S., Koehl, M.A.R., 2006. Flow in seagrass canopies: the influence of patch width. Estuar. Coast. Shelf Sci. 67, 1–9.

Fuller, A., Fan, Z., Day, C., Barlow, C., 2020. Digital twin: enabling technologies, challenges and open research. IEEE Access 8, 108952–108971.

Gacia, E., Duarte, C.M., 2001. Sediment retention by a mediterranean Posidonia oceanica meadow: the balance between deposition and resuspension. Estuar. Coast. Shelf Sci. 52, 505–514.

Ganthy, F., Soissons, L., Sauriau, P.G., Verney, R., Sottolichio, A., 2015. Effects of short flexible seagrass zostera noltei on flow, erosion and deposition processes determined using flume experiments. Sedimentology 62, 997–1023.

Giordano, R., Pluchinotta, I., Pagano, A., Scrieciu, A., Nanu, F., 2020. Enhancing nature-based solutions acceptance through stakeholders' engagement in co-benefits identification and trade-offs analysis. Sci. Total Environ. 713, 136552.

Gómez Martín, E., Costa, M.M., Egerer, S., Schneider, U.W., 2021. Assessing the long-term effectiveness of nature-based solutions under different climate change scenarios. Sci. Total Environ. 794, 148515.

Grieves, M., 2014. Digital twin: Manufacturing excellence through virtual factory replication. White Paper 1. NASA, Washington, DC, USA. Available: http://www.apriso.com.

Haine, T.W.N., Gelderloos, R., Jimenez-Urias, M.A., Siddiqui, A.H., Lemson, G., Medvedev, D., Szalay, A., Abernathey, R.P., Almansi, M., Hill, C.N., 2021. Is computational oceanography coming of Age? Bull. Am. Meteorol. Soc. 102 (8), E1481–E1493.

Hanley, M.E., Bouma, T.J., Mossman, H.L., 2020. The gathering storm: optimizing management of coastal ecosystems in the face of a climate-driven threat. Ann. Bot. 125 (2), 197–212.

Hasselmann, K., TBarnett, T.P., Bouws, E., Carlson, H., Cartwright, D.E., Enke, K., Ewing, J.A., Gienapp, H., Hasselmann, D.E., Kruseman, P., Meerburg, A., Muller, P., Olbers, D.J., Richter, K., Sell, W., Walden, H., 1973. Measurements of wind-wave growth and swell decay during the Joint North Sea Wave Project (JONSWAP). Erg¨anzungsheft zur Deutschen Hydrographischen Zeitschrift, Reihe A (8), 12 95 pp.

Hendriks, I.E., Sintes, T., Bouma, T.J., Duarte, C.M., 2008. Experimental assessment and modeling evaluation of the effects of seagrass (Posidonia oceanica) on flow and particle trapping. Mar. Ecol. Prog. Ser. 356, 163–173.

James, R.K., Silva, R., van Tussenbroek, B.I., Escudero-Castillo, M., Marino-Tapia, I., Dijkstra, H.A., et al., 2019. Maintaining tropical beaches with seagrass and algae: a promising alternative to engineering solutions. J. Biosci. 69, 136–142.

James, R.K., Lynch, A., Herman, P.M.J., van Katwijk, M.M., van Tussenbroek, B.I., Dijkstra, H.A., van Westen, R.M., van der Boog, C.G., Klees, R., Pietrzak, J.D., Slobbe, C., Bouma, T.J., 2021. Tropical biogeomorphic seagrass landscapes for coastal protection: persistence and wave attenuation during major storms events. Ecosystem 24, 301–318.

Koch, E.W., Gust, G., 1999. Water flow in tide and wave dominated beds of the seagrass Thalassia testudinum. Mar. Ecol. Prog. Ser. 184, 63–72.

Korres, G., Ravdas, M., Zacharioudaki, A., Denaxa, D., Sotiropoulou, M.., 2021. Mediterranean Sea Waves Analysis and Forecast (CMEMS MED-Waves, MedWAM3 system) (Version 1) set. Copernicus Monitoring Environment Marine Service (CMEMS). https://doi.org/10.25423/CMCC/MEDSEA_ANALYSISFORECAST_WAV_006_017_MEDWAM3.

Krause-Jensen, D., Greve, T.M., Nielsen, K., 2005. Eelgrass as a bioindicator under the european water framework directive. Water Resour. Manag. 19, 63–75.

Kumar, P., Debele, S.E., Sahani, J., Aragão, L., Barisani, F., Basu, B., Bucchignani, E., et al., 2020. Towards an operationalisation of nature-based solutions for natural hazards. Sci. Total Environ. 731, 138855.

Lei, J., Nepf, H., 2019. Wave damping by flexible vegetation: connecting individual blade dynamics to the meadow scale. Coast. Eng. 147, 138–148.

Lobeto, H., Menendez, M., Losada, I.J., 2021. Future behavior of wind wave extremes due to climate change. Sci. Rep. 11, 7869.

de los Santos, C.B., Krause-Jensen, D., Alcoverro, T., et al., 2019. Recent trend reversal for declining European seagrass meadows. Nat. Commun. 10, 3356.

Luijendijk, A., Hagenaars, G., Ranasinghe, R., Baart, F., Donchyts, G., Aarninkhof, S., 2018. The state of the World's beaches. Sci. Rep. 8, 6641.

Madsen, J.D., Chambers, P.A., James, W.F., Koch, E.W., Westlake, D.F., 2001. The interaction between water movement, sediment dynamics and submersed macrophytes. Hydrobiologia 444, 71–84.

Maicu, F., Alessandri, J., Pinardi, N., Verri, G., Umgiesser, G., Lovo, S., Turolla, S., Paccagnella, T., Valentini, A., 2021. Downscaling with an unstructured coastal-ocean model to the Goro lagoon and the Po river delta branches. Front. Mar. Sci. 8, 647781.

Marba, N., Krause-Jensen, D., Alcoverro, T., et al., 2013. Diversity of european seagrass indicators: patterns within and across regions. Hydrobiologia 704, 265–278.
Mazzella, L., Guidetti, P., Lorenti, M., Buja, M.C., Zupo, V., Scipione, M.B., Rismondo, A., Curiel, D., 1998. Biomass partionining in Adriatic Seagrass ecosystems (Posidonia Oceanica, Cymodoces Nodosa, Zostera Marina). Rapp. Comm. Int. Mer Medit. 35, 562–563.
McKenzie, L.J., Nordlund, L.M., Jones, B.L., Cullen-Unsworth, L.C., Roelfsema, C., Unsworth, R.K.F., 2020. The global distribution of seagrass meadows. Environ. Res. Lett. 15, 074041.
Meli, M., Olivieri, M., Romagnoli, C., 2021. Sea-level change along the Emilia-Romagna coast from tide gauge and satellite altimetry. Remote Sens. 13, 97.
Méndez, F.J., Losada, I.J., 2004. An empirical model to estimate the propagation of random breaking and nonbreaking waves over vegetation fields. Coast. Eng. 51, 103–118.
Méndez, F.J., Losada, I.J., Losada, M.A., 1999. Hydrodynamics induced by wind waves in a vegetation field. J. Geophys. Res. 104 (C8), 18383–18396.
Meucci, A., Young, I.R., Hemer, M., Kirezci, E., Ranasinghe, R., 2020. Projected 21st century changes in extreme wind-wave events. Sci. Adv. 6 (24), eaaz7295.
Micaletto, G., Barletta, I., Mocavero, S., Federico, I., Epicoco, I., Verri, G., Coppini, G., Schiano, P., Aloisio, G., Pinardi, N., 2021. Parallel implementation of the SHYFEM model. Geosci. Model Dev. Discuss. https://doi.org/10.5194/gmd-2021-319 [preprint in review].
Musinguzi, A., Reddy, L., Akbar, M.K., 2022. Evaluation of wave contributions in hurricane Irma storm surge hindcast. Atmosphere 13, 404.
Nepf, H., Vivoni, E., 2000. Flow structure in depth-limited, vegetated flow. J. Geophys. Res. 105 (C12), 28547–28557.
Nesshöver, C., Assmuth, T., Irvine, K.N., Rusch, G.M., Waylen, K.A., Delbaere, B., et al., 2017. The science, policy and practice of nature-based solutions: an interdisciplinary perspective. Sci. Total Environ. 579, 1215–1227.
Ondiviela, B., Losada, I.J., Lara, J.L., Maza, M., Galván, C., Bouma, T.J., van Belzen, J., 2014. The role of seagrasses in coastal protection in a changing climate. Coast. Eng. 87, 158–168.
Ondiviela, B., Galván, C., Recio, M., Jiménez, M., Juanes, J.A., Puente, A., Losada, I.J., 2020. Vulnerability of zostera noltei to sea level rise: the use of clustering techniques in climate change studies. Estuar. Coasts 43 (8), 2063–2075.
Oprandi, A., Mucerino, L., De Leo, F., Bianchi, C.N., Morri, C., Azzola, A., Benelli, F., Besio, G., Ferrari, M., Montefalcone, M., 2020. Effects of a severe storm on seagrass meadows. Sci. Total Environ. 748, 14137.
Orth, R.J., Carruthers, T.J.B., Dennison, W.C., Kendrick, C.M., Kenworthy, W.J., Olyarnik, S., Short, F.T., Waycott, M., Williams, S.L., 2006. A global crisis for seagrass ecosystems. J. Biosci. 56 (12), 987–996.
Park, K., Federico, I., Di Lorenzo, E., Ezer, T., Cobb, K.M., Pinardi, N., Coppini, G., 2022. The contribution of hurricane remote ocean forcing to storm surge along the southeastern U.S. Coast. Coast. Eng. 173, 104098.
Paul, M., Amos, C.L., 2011. Spatial and seasonal variation in wave attenuation over Zostera noltii. J. Geophys. Res. 116, C08019.
Perini, L., Calabrese, L., Salerno, G., Ciavola, P., Armaroli, C., 2016. Evaluation of coastal vulnerability to flooding: comparison of two different methodologies adopted by the Emilia-Romagna region (Italy). Nat. Hazards Earth Syst. Sci. 16, 181–194.
Pergent, G., Bazairi, H., Bianchi, C.N., Boudouresque, C.F., Buia, M.C., Calvo, S., Clabaut, P., Harmelin-Vivien, M., Mateo, M.A., Montefalcone, M., Morri, C., Orfanidis, S., Pergent-Martini, C., Semroud, R., Serrano, O., Thibaut, T., Tomasello, A., Verlaque, M., 2014. Climate change and Mediterranean seagrass meadows: a synopsis for environmental managers. Mediterr. Mar. Sci. 15 (2), 462–473.
Perini, L., Calabrese, L., Luciani, P., Olivieri, M., Galassi, G., Spada, G., 2017. Sea-level rise along the Emilia-Romagna coast (Northern Italy) in 2100: scenarios and impacts. Nat. Hazards Earth Syst. Sci. 17, 2271–2287.
Pettenuzzo, D., Large, W.G., Pinardi, N., 2010. On the corrections of ERA-40 surface flux products consistent with the Mediterranean heat and water budgets and the connection between basin surface total heat flux and NAO. J. Geophys. Res. 115, C06022.
Potouroglou, M., Bull, J.C., Krauss, K.W., Kennedy, H.A., Fusi, M., Daffonchio, D., Mangora, M.M., Githaiga, M.N., Diele, K., Huxham, M., 2017. Measuring the role of seagrasses in regulating sediment surface elevation. Sci. Rep. 1–11.
Procaccini, G., Buia, M.C., Gambi, M.C., Perez, M., Pergent, G., Pergent-Mertini, C., Romero, J., 2003. The Seagrasses of the western Mediterranean. In: Green, E.P., Short, F.T. (Eds.), World Atlas of Seagrasses. University of California, Berkeley, USA.
Rogers, W.E., Babanin, A.V., Wang, D.W., 2012. Observation-consistent input and whitecapping dissipation in a model for wind-generated surface waves: description and simple calculations. J. Atmos. Oceanic Techn. 29, 1329–1346.
Sacchi, F.C., Occhipinti, A.A., Sconfietti, R., 1990. Les Lagunes Nord-adriatiques: un environnement conservateur ouvert aux nouveautes. Bull. Soc. Zool. Fr. 114 (3), 47–60.
Sedrati, M., Ciavola, P., Reyns, J., Armaroli, C., Sipka, V., 2009. Morphodynamics of a microtidal protected beach during low wave-energy conditions. J. Coast. Res. SI56, 198–202.
Staneva, J., Alari, V., Breivik, O., Bidlot, J.R., Mogensen, K., 2017. Effects of wave-induced forcing on a circulation model of the North Sea. Ocean Dyn. 67 (1), 81–91.
Staneva, J., Grayek, S., Behrens, A., Günther, H., 2021. GCOAST: skill assessments of coupling wave and circulation models (NEMO-WAM). J. Phys. Conf. Ser. 1730, 012071.
Stankovic, M., Ambo-Rappe, R., Carly, F., Dangan-Galon, F., Fortes, M.D., et al., 2021. Quantification of blue carbon in seagrass ecosystems of Southeast Asia and their potential for climate change mitigation. Sci. Total Environ. 783, 146858.
Tanino, Y., Nepf, H., 2008. Laboratory investigation on mean drag in a random array of rigid, emergent cylinders. J. Hydraul. Eng. 134 (1), 4–41.
Telesca, L., Belluscio, A., Criscoli, A., Ardizzone, G., Apostolaki, E.T., Fraschetti, S., Gristina, M., Knittweis, L., Martin, C.S., Pergent, G., Alagna, A., Badalamenti, F., Garofalo, G., Gerakaris, V., Pace, M.L., Pergent-Martini, C., Salomidi, M., 2015. Seagrass meadows (Posidonia oceanica) distribution and trajectories of change. Sci. Rep. 5, 12505.
The WAVEWATCH III^{R} Development Group (WW3DG), 2016. User Manual and System Documentation of WAVEWATCH IIIR Version5.16, Tech. Note 329, NOAA/NWS/NCEP/MMAB, College Park, MD, USA, p. 326.
Tolman, H.L., 2014. A genetic optimization package for the Generalized Multiple DIA in WAVEWATCH III. Tech. Note 289, Ver.1.4, NOAA/NWS/NCEP/MMAB 21pp.+ Appendix.
Trotta, F., Federico, I., Pinardi, N., Coppini, G., Causio, S., Jansen, E., Iovino, D., Masina, S., 2021. A Relocatable Ocean modeling platform for downscaling to shelf- coastal areas to support disaster risk reduction. Front. Mar. Sci. 8, 642815.
Umgiesser, G., Canu, D.M., Cucco, A., Solidoro, C., 2004. A finite element model for the Venice lagoon. Development, set up, calibration and validation. J. Mar. Syst. 51 (1–4), 123–145.
UNEP (United Nations Environment Programme), 2020. Out of the Blue: The Value of Seagrasses to the Environment and to People. UNEP, Nairobi.
Waycott, M., Duarte, C.M., Curruthers, T.J.B., Orth, R.J., Dennsion, W.C., Olyarnik, S., Callandine, A., Fourqurean, J.W., Heck Jr., K.L., Hughes, A.R., Kendrick, G.A., Kenworthy, W.J., Short, F.T., Williams, S.L., 2009. Accelerating loss of seagrass across the globe threatens coastal ecosystems. Proc. Natl. Acad. Sci. 106 (30), 12377–12381.
Widdows, J., Pope, N.D., Brinsley, M.D., Asmus, H., Asmus, R.M., 2008. Effects of seagrass beds (Zostera noltii and Z. marina) on near-bed hydrodynamics and sediment resuspension. Mar. Ecol. Prog. Ser. 358, 125–126.
Yamaguchi, M., 1984. Approximate expressions for integral properties of the JONSWAP spectrum. Proc. Jpn Soc. Civ. Eng. 345, 149–152.
Young, M.A., Serrano, O., Macreadie, P.I., Lovelock, C.E., Carnell, P., Ierodiaconou, D., 2021. National scale predictions of contemporary and future blue carbon storage. Sci. Total Environ. 800, 149573.
Zhang, Y., Nepf, H., 2019. Wave-driven sediment resuspension within a model eelgrass meadow. J. Geophys. Res. Earth Surf. 124 (4), 1035–1053.
Zhang, Y.J., Gerdts, N., Ateljevich, E., Nam, K., 2019. Simulating vegetation effects on flows in 3d using an unstructured grid model: model development and validation. Ocean Dyn. 70 (2), 213230.
Zhu, Q., Wiberg, P.L., Reidenbach, M.A., 2021. Quantifying seasonal seagrass effects on flow and sediment dynamics in a back-barrier bay. J. Geophys. Res. Oceans 126, e2020JC016547.
Zieger, S., Babanin, A.V., Rogers, W.E., Young, I.R., 2015. Observation-based source terms in the third-generation wave model WAVEWATCH. Ocean Mod. 96, 2–25.